First publ. in: Science 294 (2001), pp. 1534-1537

Segregation of Nitrogen Fixation and Oxygenic Photosynthesis in the Marine Cyanobacterium *Trichodesmium*

Ilana Berman-Frank,[1]* Pernilla Lundgren,[2] Yi-Bu Chen,[1] Hendrik Küpper,[3,4,5] Zbigniew Kolber,[1] Birgitta Bergman,[2] Paul Falkowski[1]

In the modern ocean, a significant amount of nitrogen fixation is attributed to filamentous, nonheterocystous cyanobacteria of the genus *Trichodesmium*. In these organisms, nitrogen fixation is confined to the photoperiod and occurs simultaneously with oxygenic photosynthesis. Nitrogenase, the enzyme responsible for biological N_2 fixation, is irreversibly inhibited by oxygen in vitro. How nitrogenase is protected from damage by photosynthetically produced O_2 was once an enigma. Using fast repetition rate fluorometry and fluorescence kinetic microscopy, we show that there is both temporal and spatial segregation of N_2 fixation and photosynthesis within the photoperiod. Linear photosynthetic electron transport protects nitrogenase by reducing photosynthetically evolved O_2 in photosystem I (PSI). We postulate that in the early evolutionary phase of oxygenic photosynthesis, nitrogenase served as an electron acceptor for anaerobic heterotrophic metabolism and that PSI was favored by selection because it provided a micro-anaerobic environment for N_2 fixation in cyanobacteria.

Nitrogenase, the enzyme that catalyzes the reduction of atmospheric N_2 to ammonia, is irreversibly inhibited upon exposure to molecular oxygen (*1, 2*). Cyanobacteria produce molecular oxygen via photosynthesis and have evolutionary adaptations that protect nitrogenase from oxygen; these adaptations include either a temporal separation, in which N_2 fixation occurs in the dark, or a spatial segregation, in which N_2 fixation is confined to a specialized cell, the heterocyst, in which only PSI remains active. The major bloom-forming N_2-fixing organisms (diazotrophs) in modern oceans belong to the genus *Trichodesmium.* This genus is characterized by nonheterocystous filaments (trichomes), which form colonies. *Trichodesmium* are unusual among cyanobacteria because they fix nitrogen only during the photoperiod, while simultaneously producing O_2 (*3, 4*). How nitrogenase is protected from damage by photosynthetically produced O_2 and how this process is regulated has been an enigma since Dugdale *et al*. first identified these organisms as light-dependent diazotrophs 40 years ago (*3–8*). In *Trichodesmium,* nitrogenase is localized in subsets of consecutively arranged cells in each trichome, which also contain photosynthetic components (*8, 9, 10*) and comprise 15 to 20% of all cells (*9–14*). Here, we demonstrate that a combined temporal and spatial segregation of N_2 fixation and oxygen evolution provides a window of opportunity that permits the cells to fix nitrogen for only a few hours during the photoperiod.

Using fast repetition rate fluorometry (FRRF) (*15*), oxygen production, and carbon and N_2 fixation, we found that changes in the activity of photosystem II (PSII) reveal a temporal separation between N_2 fixation and photosynthesis during the photoperiod. In the field, photosynthetic carbon fixation increased in the morning but declined at midday, when nitrogenase activity peaked (Fig. 1C) (*16*). High N_2-fixation rates were measured for ~6 hours surrounding the middle of the photoperiod. When N_2 fixation declined, photosynthetic ^{14}C uptake increased again (Fig. 1A). This inverse relationship was even more pronounced in laboratory cultures, where an almost complete temporal separation of N_2 fixation and ^{14}C fixation was also observed (Fig. 2, A and C). Moreover, the period of high N_2 fixation was characterized by a decline in gross photosynthetic production, which resulted in a negative net production of oxygen (Fig. 2D). The photochemical quantum yield [variable fluorescence/maximal fluorescence (F_v/F_m)] of PSII varied inversely with N_2 fixation in both field and cultured populations (Figs. 1 and 2). During the photoperiod, F_v/F_m was 50 to 60% lower at the peak of N_2 fixation, increasing to maximum values at the end of the photoperiod, when N_2 fixation declined (Figs. 1B and 2, A and C). This characteristic diel pattern in the quantum yields was observed under both subsaturating and saturating irradiances (Figs. 1B and 2, A and C) but disappeared when N_2 fixation was inhibited in cells grown with nitrate (Fig. 2B).

We used FRRF to determine temporal changes in the redox state of photosynthetic electron transport (PET) components. The rate of oxidation of the primary electron acceptor in PSII, quinone A (Q_A^-), declined from sunrise to sunset, which suggested that the electron transfer components downstream of Q_A [e.g., at the plastoquinone (PQ) pool] are chemically reduced (Fig. 1, C and D) (*17*). The retardation of electron flow led to lower quantum yields and lower rates of photosynthetic oxygen production (Fig. 1B).

Blocking linear electron transport on the acceptor side of PSII with the inhibitors 3-3,4-dichlorophenyl-1′,1′-dimethylurea (DCMU) and 2,5-dibromo-3-methyl-6-isopropyl-*p*-benzoquinone (DBMIB), which poise the PQ pool in either an oxidized or reduced state, respectively (*18*), caused an immediate decline in nitrogenase activity when applied to cultures under aerobic conditions [Web fig. 1 (*19*)]. Under anaerobic conditions, however, nitrogenase activity was inhibited by DBMIB, which affects both photosynthetic and respiratory pathways (*20*), but was not inhibited by DCMU, which inhibits only Q_A^- oxidation. These results reveal that PET is not an immediate source of electrons for nitrogenase; dark respiration, although required for N_2 fixation, is inadequate as an oxygen-scavenging mechanism (*21*); and linear PET is required for N_2 fixation under aerobic conditions [Web fig. 2 (*19*)]. The differential effect of DCMU under aerobic and anaerobic conditions reveals that nitrogenase is protected from oxygen by electrons supplied by PSII. This phenomenon strongly implies that oxygen is scavenged by PSI via the Mehler reaction (*22*) [Web fig. 2 (*19*)].

We used fluorescently tagged primary antibodies to nitrogenase and to D1, a core protein of the oxygen-evolving PSII reaction center (*23*), to examine the pattern of segregation of N_2 fixation and oxygenic photosynthesis on a cellular level. D1 was present in most cells in a trichome, including those containing nitrogenase (Fig. 3C). Because the turnover of D1 is extremely rapid (*24*), the presence of this protein strongly implies that oxygen production and N_2 fixation are not simply spatially segregated. Moreover, when

[1]Environmental Biophysics and Molecular Ecology Program, Institute of Marine and Coastal Sciences, Rutgers University, 71 Dudley Road, New Brunswick, NJ 08901, USA. [2]Department of Botany, Stockholm University, SE–106 91 Stockholm, Sweden. [3]Photosynthesis Research Center, Institute of Microbiology, Opatovický mlýn, CZ–37981 Třeboň, Czech Republic. [4]Laboratory of Biomembranes, University of South Bohemia, Branišovská 31, CZ–370 05 České Budějovice, Czech Republic. [5]University of Konstanz, Faculty of Sciences, Department of Biology, D–78457 Konstanz, Germany.

*To whom correspondence should be addressed. E-mail: irfrank@imcs.rutgers.edu

N_2 fixation is maximal, H_2O_2 (produced primarily by the reduction of O_2 by the Mehler reaction) is present in most cells in the trichomes, including central zones where nitrogenase is clustered (*25*) (Fig. 3D).

We used a microscope equipped for two-dimensional measurement of in vivo chlorophyll fluorescence kinetics (*26*) to further examine the spatial heterogeneity in photosynthetic activity of PSII within individual cells and between trichomes. A combination of actinic radiation, saturating flashes, and a pulsed measuring light was applied to the microscopic field, enabling high spatial resolution of measured and derived fluorescence parameters for individual cells within the trichomes. In cultures measured during the early and late stages of the photoperiod, and in nitrate-grown or stationary-phase cultures, the total fluorescence yield was homogeneous in 85% of the trichomes (Fig. 3E), although zonations were observed in F_v/F_m (Fig. 3G). In nitrogen fixing cultures, total fluorescence was high (Fig. 3F) and the quantum yield of photochemistry in PSII was low (Fig. 3H). The lower quantum yields were a consequence of a proportionately larger increase in the initial dark-adapted fluorescence (F_o) than in F_m, implying that PSII reaction centers are reduced on the acceptor side (*15*). The bright inactive zones were nonuniformly distributed and were seen in whole filaments, on the tips of filaments, and in central areas of trichomes (Fig. 3F). Cells could turn photosynthetic activity (i.e., variable fluorescence) on and off within 10 to 15 min, illustrating that in *Trichodesmium,* in contrast to fully evolved heterocystous cyanobacteria, all cells are photosynthetically competent, but individual cells modulate oxygen production and consumption during the photoperiod. Moreover, the increased occurrence of inactive photosynthetic zones during the hours of high N_2 fixation is evidence of both temporal and spatial segregation of the two processes.

Our results (Figs. 1 to 3) demonstrate a combined spatial and temporal segregation of N_2 fixation from photosynthesis and suggest a sequential progression of photosynthesis, respiration, and N_2 fixation in *Trichodesmium* over a diel cycle. These pathways are entrained in a circadian pattern (*27*) that is ultimately controlled by the requirement for an anaerobic environment around nitrogenase (*28*). Light initiates photosynthesis, providing energy and reductant for carbohydrate synthesis and storage, stimulating cyclic and pseudocyclic (Mehler) electron cycling through PSI, and poising the PQ pool at reduced levels (Figs. 1A and 2, A and C) [Web fig. 2 (*19*)]. High respiration rates (*29*) early in the photoperiod (Fig. 2D) supply carbon skeletons for amino acid synthesis (the primary sink for fixed nitrogen) but simultaneously reduce the PQ pool further,

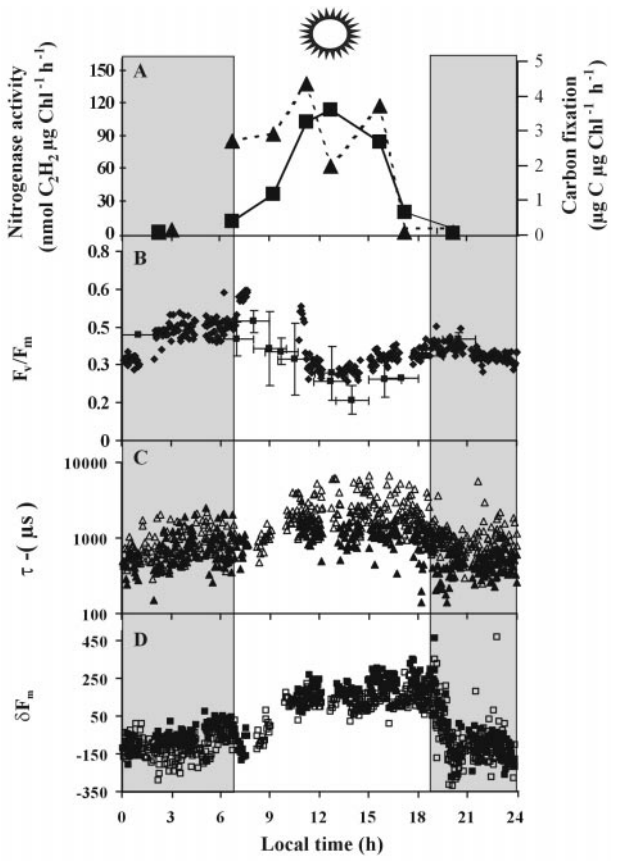

Fig 1. (**A** to **D**) Diel changes in N_2 fixation, carbon uptake, and fluorescence patterns measured by a FRRF fluorometer on surface populations of *Trichodesmium* spp. (both colonies and free filaments) collected from the Arafura and Timor Seas from 29 October to 15 November 1999. (A) Representative pattern of N_2 fixation (squares) (as measured by acetylene reduction) and acid-stable ^{14}C uptake (triangles) for *T. thiebautii* colonies obtained on 7 and 8 November 1999. (**B** to **D**) Data represent measurements made on sea water from 3 m (filtered through a 200-µm net) during 7 and 8 November (solid symbols) and 11 and 12 November (open symbols), using a continuous flowthrough FRR fluorometer. Microscopic observations showed mostly free filaments and small colonies of *Trichodesmium* spp. in these samples. (B) Photochemical quantum yields (F_v/F_m). Data shown are a composite of continuous FRRF measurements on 7 and 8 November (solid diamonds) and the average and standard deviations from the total samples of handpicked colonies between 29 October and 15 November 1999 (solid squares). (C) Oxidation rates of Q_A^- (τ). (D) Redox state of the PQ as estimated from δF_m [$\delta F_m = F_m$ (ST – MT)].

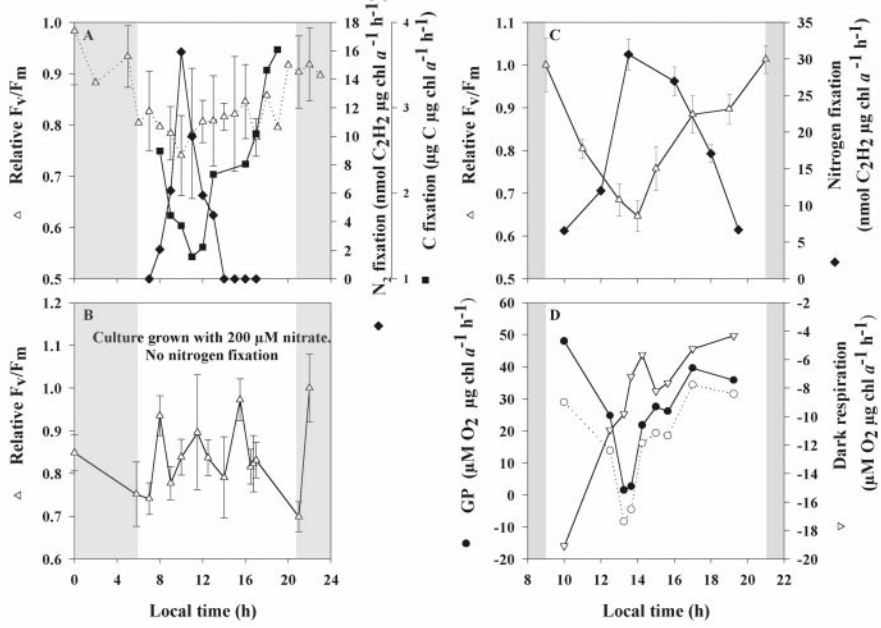

Fig. 2. Diel patterns in N_2 fixation, in quantum efficiencies of PSII and in respiratory oxygen consumption and photosynthetic oxygen evolution in cultures of *Trichodesmium* strain IMS101. (**A** and **B**) Axenic cultures grown under a 14:10 hour light/dark cycle (L/D) under 40 µmol of quanta m^{-2} s^{-1}. (**C** and **D**) Culture grown at 12:12 L/D under 80 µmol of quanta m^{-2} s^{-1}. (A and C) Quantum yields (triangles) and acetylene reduction rates (diamonds) of culture grown under diazotrophic conditions with no inorganic nitrogen source. (B) Quantum yields (triangles) of culture grown on 200 µM NO_3 exhibiting no N_2 fixation as measured by the acetylene reduction method. (D) Oxygen consumption and evolution as measured on a Clark-type O_2 electrode. Dark respiration (triangles), gross photosynthesis (circles), and net oxygen evolution (open circles).

sending negative feedback to linear PET [Web fig. 2 (*19*)]. The reduced PQ pool leads to a down-regulation of PSII (Figs. 3, F and H, and 1, C and D). However, linear electron flow to PSI is never abolished [Web fig. 2 (*19*)]. The down-regulation of PSII opens a window of opportunity for N_2 fixation during the photoperiod, when oxygen consumption exceeds oxygen production. As the carbohydrate pool is consumed, respiratory electron flow through the PQ pool diminishes, intracellular oxygen concentrations rise, the PQ pool becomes increasingly oxidized, and net oxygenic production exceeds consumption (Figs. 1A and 2, C and D). Nitrogenase activity is lost until the following day.

The combination of spatial and temporal segregation of N_2 fixation and oxygenic photosynthesis during the photoperiod appears to reflect the evolutionary history of N_2 fixation in cyanobacteria. Nitrogenase is an ancient enzyme that almost certainly arose in the Archean Ocean before the oxidation of the atmosphere by oxygenic photoautotrophs (*30, 31*). We propose that under the prevailing anaerobic conditions of that period in Earth's history, N_2 served as a readily accessible electron sink for anaerobic heterotrophs. In contemporary diazotrophic microbes, including cyanobacteria, the reductants for nitrogenase are provided by respiratory electron flow. With the evolution of cyanobacteria and the subsequent generation of molecular oxygen, oxygen-protective mechanisms in diazotrophs would be essential. Indeed, phylogenetic trees of diazotrophic cyanobacteria, based on nifH gene sequences, suggest that *Trichodesmium* branched out very early (*32*). A full temporal separation, in which nitrogen is only fixed at night, then developed in unicellular cyanobacterial diazotrophs and in some nonheterocystous filamentous diazotrophs (*7*). Finally, in yet other filamentous organisms, complete segregation of N_2 fixation and photosynthesis was achieved with the cellular differentiation and evolution of heterocystous cyanobacteria (*33*). It is remarkable that the pathway adopted by *Trichodesmium* has persisted in the oceans through the present time. This persistence suggests that the tempo of evolution in marine diazotrophic cyanobacteria is extremely slow.

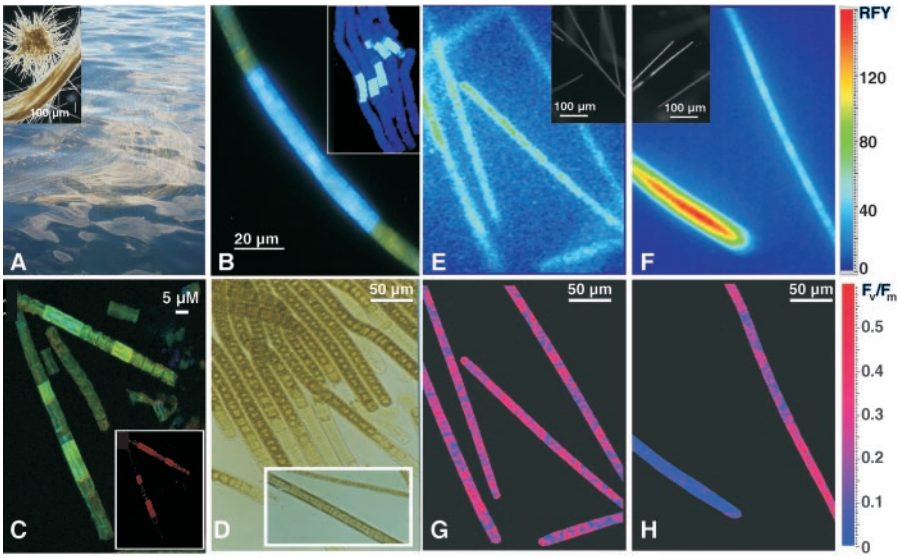

Fig 3. (**A**) A surface bloom of *Trichodesmium* spp. from the Arafura Sea. Inset: Puff and tuft formations of *T. thiebautii* colonies. (**B**) Nitrogenase localization in a single IMS101 trichome visualized with an epifluorescent microscope (Olympus U-MWU; BP 330 to 385, DM 400, BA 420) using a fluorescent secondary antibody Alexa-350 (Molecular Probes). Insert: Natural population of *T. erythraeum* probed as above. (**C**) *Trichodesmium* IMS101 probed simultaneously with fluorescently tagged primary antibodies to both D1 and nitrogenase and viewed on a confocal laser microscope (Zeiss LSM410) at 488/528 nm and 568/600 to 620 bandpass excitation/emission for D1 (green) and nitrogenase (red), respectively. **The** large image is the composite overlay of both channels. Insert: Nitrogenase label only. (**D**) Colonies of *T. erythraeum*, collected from surface waters of the Arafura Sea and stained with DAB, showing the intracellular distribution of H_2O_2 as a brown stain throughout the cells during peak hours of N_2 fixation (13:30 to 14:30). Insert: Midsection of a single trichome stained with brown deposits. (**E** to **H**) Trichomes of cultured *Trichodesmium* IMS101 viewed with a microscope for two-dimensional measurements of in vivo chlorophyll fluorescence kinetics (*45*). (E and G) Trichomes from the early hours (00:00 to 04:00) of the photoperiod when N_2 fixation is low. (F and H) Trichomes from hours of high N_2 fixation (5 to 7 hours into the photoperiod). (E and F) Total chlorophyll fluorescence. Inserts: Trichomes photographed with a nonamplified high-resolution camera showing the pattern of normal and bright filaments (i.e., high total fluorescence to very low F_v/F_m) for the corresponding sampling times. Scale bar indicates relative fluorescence yield. (G and H) False color images of the two-dimensional distribution of PSII efficiency, F_v/F_m along the trichomes.

References and Notes

1. P. W. Ludden, G. P. Roberts, in *Anoxygenic Photosynthetic Bacteria*, R. E. Blankenship, M. T. Madigan, C. E. Bauer, Eds. (Kluwer Academic, Dordrecht, Netherlands, 1995), pp. 929–947.
2. In cyanobacteria, nitrogenase consists of two proteins: the iron protein and the iron-molybdenum protein. The former is an α_2 dimer with a molecular weight (MW) of about 65,000 that contains a single Fe_4S_4 cluster bound between subunits. The latter is an $\alpha_2\beta_2$ heterotetramer, of approximate MW of 250,000 with each unit containing two types of clusters, the P cluster and the FeMoco center (sometimes called the M cluster). The P cluster is an Fe_8S_7 center that functions as a conduit for electron transfer, accepting electrons from the Fe_4S_4 cluster of the iron protein [in conjunction with adenosine triphosphate (ATP) hydrolysis] and donating them to the FeMoco center, which is the site of N_2 reduction. Whereas both the Fe_4S_4 and P clusters are inactivated by O_2, the Fe_4S_4 cluster is much more susceptible and irreversibly damaged (*34*).
3. R. C. Dugdale *et al.*, *Deep Sea Res.* **7**, 297 (1961).
4. T. Saino, A. Hattori, *Deep Sea Res.* **25**, 1259 (1978).
5. E. J. Carpenter, C. C. Price, *Science* **191**, 1278 (1976).
6. D. G. Capone *et al.*, *Science* **276**, 1221 (1997).
7. B. Bergman *et al.*, *FEMS Microbiol. Rev.* **19**, 139 (1997).
8. H. W. Paerl, *J. Phycol.* **30**, 790 (1994).
9. S. J. Lin *et al.*, *App. Environ. Microbiol.* **64**, 3052 (1998).
10. B. Bergman, in *Marine Nitrogen-Fixing Cyanobacteria*, L. Charpy, T. Larkum, Eds. (Marine Cyanobacteria, Bulletin Institute Oceanographic, Monaco, 1999), pp. 158–163.
11. S. Janson *et al.*, *FEMS Microbiol. Lett.* **118**, 9 (1994).
12. C. Fredriksson, B. Bergman, *Microbiology* **141**, 2471 (1995).
13. ———, *Protoplasma* **197**, 76 (1997).
14. Primary NifH antibody was raised in rabbit against the Fe protein from *Rhodospirillum rubrum* and was visualized with an epifluorescent microscope (Olympus BX-60 ultraviolet light) [excitation filter (BP) 330 to 385, dichroic mirror (DM) 400, barrier filter (BA) 420 nm] by using a secondary antibody coupled to Alexa-350 (Molecular Probes).
15. FRRF measures fluorescence transients induced by a series of subsaturating excitation pulses (*35*). F_o is measured when Q_A is fully oxidized; F_m occurs when Q_A is fully reduced. $F_v = (F_m - F_o)$, and the photochemical quantum yield of PSII (F_v/F_m) (*36*) correlate well with independent measurements of photosynthetic competence such as yield of oxygen evolution (*37*).
16. Field populations of *Trichodesmium erythreum* and *T. thiebautii* were collected and analyzed in the Arafura and Timor Seas, north of Australia, between 21 October and 16 November 1999. Colonies and filaments were obtained with net tows at varying depths, hand-picked, and resuspended in filtered sea water. For continuous FRRF measurements sea water was pumped from a 3-m depth and filtered through 200-µm mesh before entering the FRRF at a flow of 240 ml/min *Trichodesmium* species composition was monitored microscopically.
17. $\delta F_m = F_m(ST - MT)$, where ST and MT are single- and multiple-turnover flashes, respectively (*15*).
18. DCMU binds competitively with the secondary quinone acceptor (Q_B) and prevents the reduction of the PQ. DBMIB prevents the oxidation of the PQ by blocking the plastoquinol binding site of cytochrome b_6f (*38*).].
19. Supplementary Web material is available on *Science* Online at www.sciencemag.org/cgi/content/full/294/5546/1534/DC1.
20. In cyanobacteria, NAD(P)H carries electrons produced by respiratory oxidation into the photosynthetic electron transport chain via the thylakoid-bound dehydrogenase(s), which subsequently reduces the PQ and the cytochrome b_6f complex, which is a plastoquinol oxidoreductase and lies downstream of the PQ just before reaching PSI. Thus, DBMIB inhibits both photosynthetic and respiratory electron flow downstream of cytochrome b_6f (*39*).

21. Local zones of higher respiratory activity may be important, however, as evidenced by higher levels of the respiratory enzyme cytochrome oxidase in the subsets of cells with nitrogenase than in those without (*40*). Deployment of oxygen and reactive oxygen species detoxification systems (such as Mehler, thioredoxin peroxidases, and catalase) also aid in providing a microanaerobic environment around cells fixing nitrogen. Colony formation may further reduce ambient oxygen concentrations (*5, 8*), enabling the higher N_2 fixation rates (per unit of chlorophyll a) observed in colonies as compared to single trichomes (*41*).
22. In mature heterocysts, PSI is the only active photosynthetic reaction center and is important in providing the extra ATP for N_2 fixation through cyclic electron transport. In *Trichodesmium*, high Mehler activity has also previously been invoked in supplying ATP (*42, 43*).
23. Antibodies to D1 fragments and to dinitrogenase reductase raised in rabbits were conjugated to fluorescent probes Alexa 488 and Alexa 568, respectively (Molecular Probes) and labeled sequentially (nitrogenase followed by D1) in cells fixed in 100% ethanol and permeabilized with 0.5% dimethyl sulfoxide in phosphate buffer. Samples were viewed on a confocal laser microscope (Zeiss LSM410) at 488/528 nm and 568/600 to 620 nm bandpass excitation/emission for the D1 and nitrogenase, respectively. The results obtained for cultures grown in several conditions and at several points during the diel cycle show that D1 occurs in most cells in a trichome and co-occurs in the same cells as nitrogenase.
24. Z. Krupa, G. Öquist, P. Gustafsson, *Plant Physiol*. **93**, 1 (1990).
25. *Trichodesmium* colonies were stained with 3,3-diaminobenzidine (DAB), which polymerizes, in the presence of peroxidases, with intracellular H_2O_2 produced by reduction of oxygen in PSI, to form brown deposits (*44*). The final concentration of DAB used was 1 mg/ml. No external peroxidases were added, indicating the presence of active peroxidases involved in the antioxidative pathways [Web fig. 2 (*19*)]. Negative controls of dark-incubated *Trichodesmium* trichomes showed low DAB staining throughout the trichomes.
26. Trichomes were filtered, embedded in 1% agarose (melting point 25°C) in sea water, and placed in a cellophane-sealed thermostated chamber pumped through with medium (100 ml min^{-1} at 25°C, saturated with air). To reduce artifacts caused by handling, fresh samples were prepared for each time point. Samples were viewed with a microscope for two-dimensional measurements of in vivo chlorophyll fluorescence kinetics (*45*). Measurements were done with 30-μs flashes of nonactinic measuring light, 1000 μmol of quanta m^{-2} s^{-1} of actinic light, and 10,000 μmol of quanta m^{-2} s^{-1} saturating multiturnover flashes. Fluorescence kinetics were measured simultaneously on 300 $\times$ 400 pixels.
27. A circadian pattern temporally separates the abundance of mRNA for nifH (nitrogenase), psbA (encoding for PSII) and psaB (encoding for PSI) in *Trichodesmium* strain IMS101 (*46, 47*).
28. In *Trichodesmium*, high external concentrations of molecular oxygen affect nitrogenase activity within ~15 min (*48*), whereas Western and Northern blots of nitrogenase and nifH (*49*) revealed that the enzyme and transcript levels are not much affected 2 hours after addition of DCMU and DBMIB, indicating that the loss of activity is not due to the loss of the enzyme but rather to a posttranslational inactivation of the enzyme by oxygen.
29. In most cyanobacteria, dark respiration rates are generally $<$10% of the gross oxygen evolution rates (*50*). In *Trichodesmium*, dark respiration ranged from 13 to 46% of the maximum gross oxygen evolution rate, with a mean of 23% and consisting, in the dark, of approximately 30% of the absolute magnitude of maximal gross photosynthesis. Moreover, at low light intensities (typical of those found for depth-adapted populations or cultured populations), more oxygen was consumed than evolved (*51, 52*).
30. Phylogenetic analyses suggest a single ancestral origin for the catalytic subunits of the enzyme complex responsible, namely nitrogenase (*53*).
31. P. G. Falkowski, *Nature* **387**, 272 (1997).
32. J. P. Zehr, M. T. Mellon, S. Zani, *Appl. Environ. Microbiol*. **64**, 3444 (1998).
33. C. P. Wolk, A. Ernst, J. Elhai, in *The Molecular Biology of Cyanobacteria,* D. E. Bryant, Ed. (Kluwer Academic, Dordrecht, Netherlands, 1994), pp. 769–823.
34. B. K. Burgess, D. J. Lowe, *Chem. Rev*. **96**, 2983 (1996)
35. Z. Kolber, O. Prašil, P. G. Falkowski, *Biochim. Biophys. Acta* **1367**, 88 (1998).
36. G. H. Krause, E. Weis, *Annu. Rev. Plant Physiol. Plant Mol. Biol*. **42**, 313 (1991).
37. D. Campbell *et al.*, *Microbiol. Mol. Biol. Rev*. **62**, 667 (1998).
38. P. G. Falkowski, J. A. Raven, *Aquatic Photosynthesis* (Blackwell Science, Malden, MA, ed. 1, 1997).
39. M. Hirano, K. Satoh, S. Katoh, *Photosyn. Res*. **1**, 149 (1980).
40. B. Bergman *et al.*, *Appl. Environ. Microbiol*. **59**, 3239 (1993).
41. R. M. Letelier, D. M. Karl, *Aquatic Microbiol Ecol*. **15**, 265 (1998).
42. T. M. Kana, in *Marine Pelagic Cyanobacteria: Trichodesmium and Other Diazotrophs*, E. J. Carpenter, Ed. (Kluwer Academic, Dordrecht, 1992), pp. 29–41.
43. _____, *Limnol. Oceanogr*. **38**, 18 (1993).
44. H. Thordal-Christensen *et al*., *Plant J*. **11**, 1187 (1997).
45. H. Küpper, I. Šetlik, M. Trtilek, L. Nedbal, *Photosynthetica* **38,** 553 (2000).
46. Y. B. Chen *et al*., *J. Bacteriol*. **180**, 3598 (1998).
47. _____, *Plant Mol. Biol*. **41,** 89 (1999).
48. P. Lundgren, Y. Gerchman, unpublished data.
49. I. Berman-Frank *et al*., unpublished data.
50. J. C. P. Matthijs, H. J. Lubberdin, in *Biochemistry of the Algae and Cyanobacteria*, *Proc. Phytochem. Soc. Eur.* (Clarendon, 1988) pp. 131-145.
51. T. Roenneberg, E. J. Carpenter, *Mar. Biol*. **117**, 693, (1993).
52. E. J. Carpenter, T. Roenneberg, *Mar. Ecol. Prog. Ser*. **118**, 267 (1995).
53. J. P. Zehr, E. J. Carpenter, T. A. Villareal, *Trends Microbiol*. **8**, 68 (2000).
54. We thank D. Capone, E. Carpenter, and the captain and crew of the R/V *Ewing* for enabling the field study; R. Dotson for setting up the continuous flow to the FRR fluorometer; K. Bateman (Stockholm University) and K. Wyman (Rutgers University) for technical assistance; J. Waterbury (Woods Hole Oceanography Institute) for providing axenic cultures, lab space, invaluable help, and ideas; P. Ludden (University of Wisconsin), S. Nordlund (Stockholm University), and A. Matoo (U.S. Department of Agriculture) for their gift of antibodies; O. Prašil, I. Šetlik, and the Microbiological Institute, Trebon, for hosting I.B.-F. [Czech (CZ)-NSF grant ME379 and Ministry of Education of the Czech Republic grant MSM 12310001] and providing access to the kinetic microscope, which was built in cooperation with Photon Systems Instruments, Czech Republic. Supported through grants to P.F. from the U.S. Department of Energy Office of Science program for Research on Ocean Carbon Sequestration, the Center for Bioinorganic Chemistry (Princeton University), NASA Earth System Science Program; to B.B. from the Swedish Foundation for International Cooperation in Research and Higher Education and the Swedish Natural Science Research Council (SIDA/SAREC); and to H. K. from Studienstiftung des Deutschen Volkes.